

# METHODS USED IN INCREASED RESOLUTION PROCESSING

## *Polygon Based Interpolation and Robust Log-polar Based Registration*

Stéfan van der Walt and Ben Herbst  
*University of Stellenbosch, South Africa*

Keywords: Geometry, interpolation, registration, image-processing, astronomy, log-polar transform.

Abstract: A polygon-based interpolation algorithm is presented for use in stacking RAW CCD images. The algorithm improves on linear interpolation in this scenario by closely describing the underlying geometry. 25 frames are stacked in a comparison. When stacking images, it is required that these images are accurately aligned. We present a novel implementation of the log-polar transform that overcomes its prohibitively expensive computation, resulting in fast, robust image registration. This is demonstrated by registering and stacking CCD frames of stars taken by a telescope.

## 1 INTRODUCTION

In this paper we describe two techniques which have proved useful in the construction of resolution refining algorithms. The first is polygon-based interpolation. When stacking RAW CCD readouts, the frames are aligned and interpolation is applied to obtain values on a common grid. Unlike bi-linear interpolation, that can cause blur and is not well suited to the geometry of the problem, geometric interpolation is designed to take not only the positions but also the *shape* of pixels into account.

The second technique is image registration or alignment using the log-polar transform (LPT). While the LPT has been proposed for this purpose before, the computational cost is prohibitive. We show how the LPT can be used in a way that requires much fewer computations, without compromising robustness or accuracy.

## 2 POLYGON-BASED INTERPOLATION

Given an image, or grid of pixel values, we would like to calculate the value at an arbitrary point in the grid. Bi-linear interpolation essentially uses a weighted av-

erage of the closest four pixels, based on their distances from the target position (Press et al., 2003). If pixels are seen as infinitely small points in space, this method yields accurate results.

When, however, we consider that pixels have finite areas, this method is only reasonably accurate when the target pixel is horizontally and vertically aligned with the original grid. As soon as rotation or skew comes into play, linear interpolation no longer resembles the underlying geometry, as is the case when stacking raw CCD frames. The CCD sensor comprises a number of light-sensitive capacitors, arranged in a grid. For the purpose of this article we will assume that the shape of these capacitors is square, but the method described allows for any geometry, also in the arrangement on the sensor itself (permitted that there are no holes, as in the case of the colour-masked CCD).

Given a target pixel position,  $(r, s)$ , and a transformed (for example rotated and translated) source pixel at  $(m, n)$  with value  $W_{m,n}$ , we would like to calculate the contribution of the source to the target. We construct a quadrilateral polygon at the target position with vertices

$$\begin{bmatrix} x_t & = & s & s+1 & s+1 & s \\ y_t & = & r & r & r+1 & r+1 \end{bmatrix}$$

van der Walt S. and Herbst B. (2007).

METHODS USED IN INCREASED RESOLUTION PROCESSING - Polygon Based Interpolation and Robust Log-polar Based Registration.

In *Proceedings of the Second International Conference on Computer Vision Theory and Applications - ICFIA*, pages 135-140

Copyright © SciTePress

as well as at the reference position with vertices

$$\begin{bmatrix} x_r & = & n & n+1 & n+1 & n \\ y_r & = & m & m & m+1 & m+1 \end{bmatrix}.$$

The vertices  $x_r$  and  $y_r$  are then inversely transformed to align with the target grid. The source pixel value is weighted with the area of the polygon intersection between source and target pixels (see Fig. 1). This method has the advantage that it can be adapted accurately for any kind of spatial transformation, although it may require adding more vertices to support non-linear transformations.

Using this technique, 25 frames provided by the NASA Pathfinder mission were stacked (Peter Cheeseman and Bob Kanefsky and Richard Kraft and John Stutz and Robin Hanson, 1996). The frames were aligned using localised features (Jianbo Shi and Carlo Tomasi, 1994), with trivial outlier rejection. A high-resolution grid was specified after which the polygon intersections were calculated using the Liang-Barsky algorithm (You-Dong Liang and Brian A. Barsky, 1983). The results are shown in Fig. 2. Note that this is *not* a super-resolution algorithm (although the interpolation can certainly be combined with such a statistical estimation process), but simply increased resolution stacking.

### 3 REGISTRATION

Registration algorithms can be divided into two broad classes: those that operate in the spatial and frequency (i.e. Fourier) domains, respectively. In the spatial domain, there are sparse methods including local descriptors, that depend on some form of feature extraction, and dense methods that operate directly on image values such as optical flow and correlation. The two classes generally differ in that the spatial methods are localised, whereas the frequency domain methods (Reddy and Chatterji, 1996; Hanzhou Liu and Baolong Guo and Zongzhe Feng, 2006; Hassan Faroosh (Shekarforoush) and Josiane B. Zerubia, 2002; Harold S Stone and Stephen A Martucci and Michael T Orchard and Ee-chien Chang, 2001) operate globally. Attempts have been made to bridge this gap, by using wavelet and other transforms to locate information-carrying energy (George Lazardis and Maria Petrou, 2006). These have been met with varying success.

Each registration method has its own particular advantages and disadvantages. Fourier methods, for example, are fast but inaccurate, suffer from re-sampling and occlusion effects (Siavash Zokai and George Wolberg, 2005, p. 1425), and only operate

globally. Iterative registration, on the other hand, is highly accurate but extremely slow, and prone to mis-registration due to local minima in the minimisation space.

These problems led to the development of methods based on localised interest points (Carlo Tomasi and Takeo Kanade, 1991; Jianbo Shi and Carlo Tomasi, 1994; Tommasini et al., 1998; Tony Lindeberg, 1998), such as the scale-invariant feature transform (SIFT) (Lowe, 2003), the fast Speeded Up Robust Features (SURF) (Herbert Bay and Tinne Tuytelaars and Luc Van Gool, 2006) and others (K. Mikolajczyk and C. Schmid, 2002). All these methods depend on unique localised features, which are available in many images. There are, however, cases where it is very difficult to distinguish one feature from another without examining its spatial context.

As an example, we will use frames recorded by a CCD mounted on a telescope pointing at a deep-space object. It is very difficult to find features to track in these images, because the stars (all potential features) are virtually identical and rotationally invariant. Since local features fail, and global methods are slow and unreliable, we would like to find an algorithm that can bridge the gap.

We will proceed to show that the log-polar transform (LPT) is an ideal candidate. While previously its use has been limited due to its high computational cost, we develop ways of reducing those costs and making the LPT behave more like local features.

### 4 THE LOG POLAR TRANSFORM

The log-polar transform (LPT) spatially warps an image onto new axes, angle ( $\theta$ ) and log-distance ( $L$ ). Pixel coordinates  $(x, y)$  are written in terms of their offset from the centre,  $(x_c, y_c)$ , as

$$\begin{aligned} \bar{x} &= x - x_c \\ \bar{y} &= y - y_c. \end{aligned}$$

For each pixel, the angle is defined by

$$\theta = \begin{cases} \arctan\left(\frac{\bar{y}}{\bar{x}}\right) & \bar{x} \neq 0 \\ 0 & \bar{x} = 0 \end{cases}$$

with a distance of

$$L = \log_b\left(\sqrt{\bar{x}^2 + \bar{y}^2}\right).$$

The base,  $b$ , which determines the width of the transform output, is chosen to be

$$b = e^{\ln(d)/w} = d^{\frac{1}{w}},$$

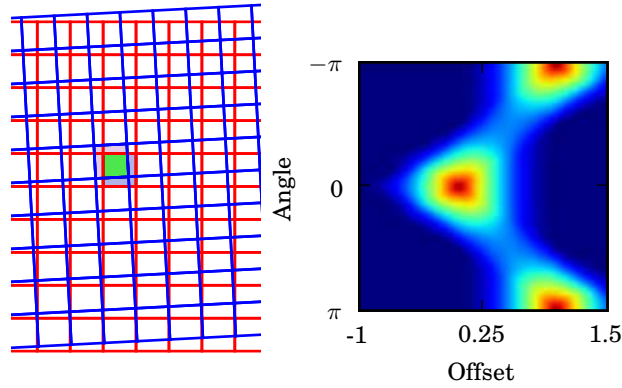


Figure 1: Illustration of the relation between interpolation weight and polygon overlap. A single polygon was transformed with the given offset and angle to obtain the shown overlap, where blue represents zero and red represents one. Note that, unlike with linear interpolation, the weights not only depend only on the distances between points.

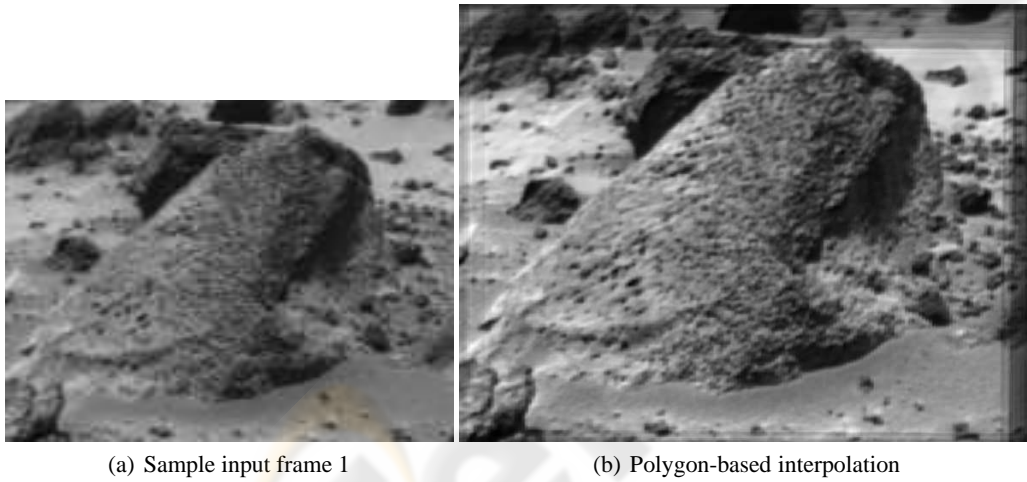


Figure 2: Enhanced resolution obtained by stacking 25 frames, using polygon-based interpolation.

where  $d$  is the distance from  $(x_c, y_c)$  to the corner of the image, and  $w$  is the width or height of the input image, whichever is largest.

When warping images, it is not possible to use the forward transform. Since we use discrete coordinates (integer  $x$  and  $y$  values), more than one input coordinate may map to the same output coordinate. Worse still, not every output coordinate will be covered.

One solution is to calculate the irregular grid of coordinates obtained by transforming each input coordinate (without discretising). Then, the input is warped and resampled (using interpolation) at the required output positions. An easier and computationally less intensive method is to reverse the process. For each output coordinate, the transformation is applied in reverse, to obtain a coordinate in the input image. Using interpolation, an output value is deter-

mined from the input. This can be done if, ignoring the effect of discretisation, the transformation function is a one-to-one correspondence, and all input and output coordinates are mapped.

Given  $\theta$  and  $L$ , we would now like to find  $x$  and  $y$ . First, calculate the distance  $r$  from the centre,

$$\begin{aligned} r &= e^{\ln(b)L} \\ &= e^{L \ln(d)/w} \end{aligned}$$

after which  $x$  and  $y$  can be recovered as

$$\begin{aligned} x &= r \cos(\theta) + x_c \\ y &= r \sin(\theta) + y_c. \end{aligned}$$

Note the relationship of the input image to the axes of the LPT: if the input is rotated it results in a shift in the  $\theta$  axis, whereas scaling the input is seen as a shift

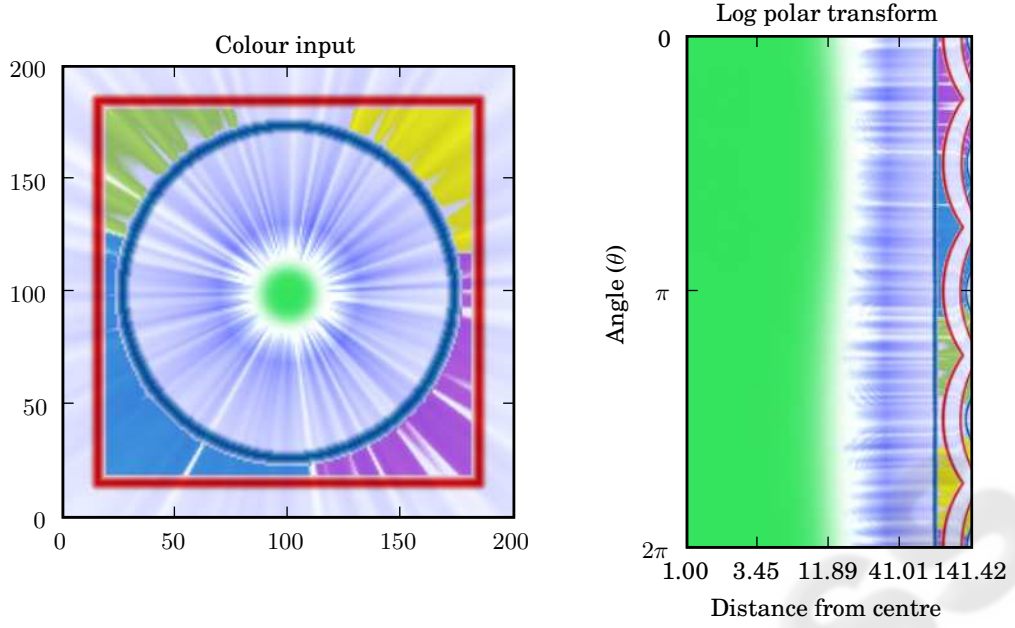


Figure 3: Illustration of the log-polar transform.

in the  $L$  axis. It is this property of the LPT that is used in registration.

## 5 FAST REGISTRATION BASED ON THE LOG-POLAR TRANSFORM

In (Siavash Zokai and George Wolberg, 2005), affine registration based on the log-polar transform is described. Given a reference frame,  $R(x,y)$ , and a target frame,  $B(x,y)$ , we want to find a transformation,  $T$ , such that

$$R(x,y) = B(T(x,y)).$$

Assuming that the frames are images taken of the same object from a long distance, we know that the transformation must be a similarity, i.e. it is limited to translation, rotation and scale. If we express a coordinate  $(x,y)$  as a homogenous coordinate  $\mathbf{p} = [x,y,1]^T$ , we can view the transformation as a matrix multiplication,

$$T(\mathbf{p}) = M\mathbf{p}$$

where

$$M = \begin{bmatrix} s\cos(\theta) & -s\sin(\theta) & t_x \\ s\sin(\theta) & s\cos(\theta) & t_y \\ 0 & 0 & 1 \end{bmatrix} = \left[ \begin{array}{c|c} sR & \mathbf{t} \\ \hline \mathbf{0}^T & 1 \end{array} \right]$$

and  $R$  represents rotation,  $\mathbf{t}$  translation and  $s$  scale. The LPT proceeds as follows:

- From the centre of the reference frame,  $\mathbf{p}_r = [x_r, y_r]^T$ , cut a disc with a radius of roughly 20% of the image width (larger or equal to the size of the features we wish to track), and obtain its LPT.
- For each position in the target frame,  $\mathbf{p}_t = [x_t, y_t]^T$ , cut out a disc of the same size as the reference disc and obtain its LPT. Correlate the result with the reference disc, taking care to wrap the angles-axis. This is easily accomplished using the FFT. If the normalised correlation is higher than at any other point thus far, store the position, rotation ( $\theta$ ) and scale ( $s$ ).

The  $s$  and  $R$  components of  $M$  can now be determined, after which the position is related to translation by

$$\mathbf{t} = \mathbf{p}_r - sR\mathbf{p}_t.$$

The method outlined above is extremely robust, even in the presence of high levels of noise, changes in illumination and large differences in scale, rotation and translation. Unfortunately, its computational complexity proves to be prohibitive: even for a small image of dimension  $200 \times 200$ , roughly 40000 log-polar transforms and correlations need to be calculated. Furthermore, unless the target frame overlaps with the centre of the reference frame, the registration fails.

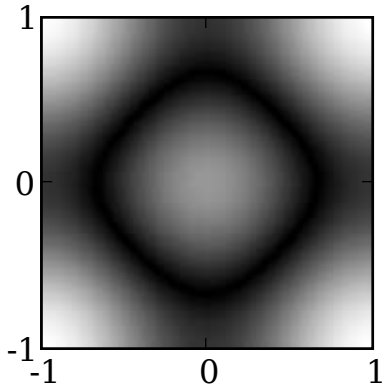


Figure 4: Fourier domain representation of the high-frequency emphasis kernel.

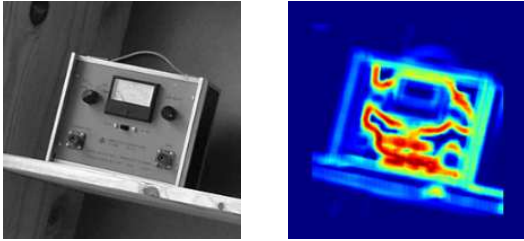


Figure 5: The variance map highlights areas of interest.

To address this problem, we choose *more* discs in the reference frame, but severely limit the number of discs in the target frame, thereby reducing the number of log-polar transforms and correlations that need to be calculated. To accomplish this, we need to identify areas in both the reference and target frames that are likely to contain useful features. Smooth areas are less likely to contain such information. An intuitive measure of smoothness is variance—as is often used in texture analysis—but this commonly fails. For example, imagine two images, one being a checkerboard pattern and the other divided in two halves, one black and one white. The intensities in these images will have the same variance, while their content and texture differs. To counter this problem, we first apply the high-frequency emphasis kernel,

$$\kappa = \begin{bmatrix} 0 & 1 & 0 \\ 1 & -1 & 1 \\ 0 & 1 & 0 \end{bmatrix},$$

of which the frequency response is shown in Figure 4, to each frame. The variance is then calculated over a moving window, yielding a map indicating potentially useful features, as shown in Figure 5.

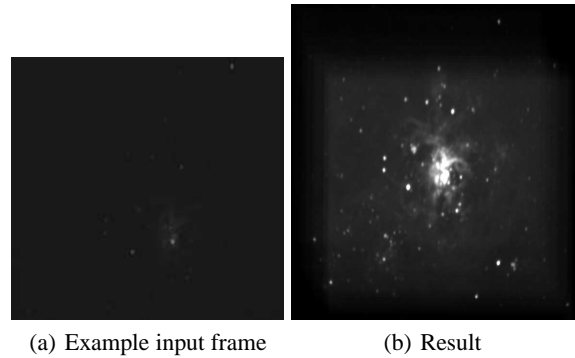


Figure 6: Stacking is often used in astronomy to limit noise and gather more light on the camera sensor. Here, 25 observations are stacked after automatic registration, using the log-polar algorithm (photographs by Chris Forder of the Cederberg Observatory).

To locate the position of such features, the map is divided into smaller blocks, and the peak value in each block is taken as the position of a disc. We use 16 equally-sized blocks in the reference frame and 40 equally-sized blocks in each of the target frames. Positions are rejected when the variance falls outside the range of variances at reference positions. Discs can also be rejected in terms of other criteria, for example on the grounds of being symmetric, since such discs can yield invalid matches at different angles. The process outlined earlier is then followed, correlating discs in the reference and target frames to find the registration parameters. Note that the number of log-polar transforms and correlations are reduced from tens-of-thousands to fewer than 160. All log-polar transforms use the same set of transformation coordinates, which only need to be calculated once.

Since the variance map has a smoothing effect on the input, we have to allow for a small error in the position of maximum correlation. A small search area, typically  $5 \times 5$  pixels, is defined around this point, for which the registration is repeated to provide a refined measurement.

It is suggested in (Siavash Zokai and George Wolberg, 2005) that iterative minimisation of the registration parameters is performed, thereby increasing the accuracy even further. We have found, however, that this process often diverges due to the large number of local minima in the minimisation space.

Figure 6 shows 25 frames from a telescope CCD registered and stacked.

## 6 CONCLUSION

Linear interpolation is not equally well suited to all applications. We show that an algorithm that is closely related to the underlying geometry of an application can yield results with higher accuracy.

For most applications in registration, localised interest points provide fast, localised and accurate results. However, there are cases where these algorithms fail, thus requiring a more robust algorithm. The log-polar transform provides such an algorithm, at significant computational cost. Using the methods described in this paper, the computational cost of LPT-based registration can be decreased, making it both practical and effective.

## REFERENCES

- Carlo Tomasi and Takeo Kanade (1991). Detection and Tracking of Point Features. Technical Report CMU-CS-91-132, Carnegie Mellon University.
- George Lazardis and Maria Petrou (2006). Image Registration Using the Walsh Transform. *IEEE Transactions on Image Processing*, 15(8):2343–2357.
- Hanzhou Liu and Baolong Guo and Zongzhe Feng (2006). Pseudo-Log-Polar Fourier Transform for Image Registration. *IEEE Signal Processing Letters*, 13(1):17–20.
- Harold S Stone and Stephen A Martucci and Michael T Orchard and Ee-chien Chang (2001). A fast direct Fourier-based algorithm for subpixel registration of images. *IEEE Transactions on Geoscience and Remote Sensing*, 39(10):2235–2243.
- Hassan Faroosh (Shekarforoush) and Josiane B. Zerubia (2002). Extension of Phase Correlation to Subpixel Registration. *IEEE Transactions on Image Processing*, 11(3):188–200.
- Herbert Bay and Tinne Tuytelaars and Luc Van Gool (2006). SURF: Speeded Up Robust Features. In *Proceedings of the ninth European Conference on Computer Vision*.
- Jianbo Shi and Carlo Tomasi (1994). Good Features to Track. In *IEEE Conference on Computer Vision and Pattern Recognition*, pages 593–600.
- K. Mikolajczyk and C. Schmid (2002). An Affine Invariant Interest Point Detector. In *ECCV I*, number 128–142.
- Lowe, D. (2003). Distinctive image features from scale-invariant keypoints. *International Journal of Computer Vision*, 20:91–110.
- Peter Cheeseman and Bob Kanefsky and Richard Kraft and John Stutz and Robin Hanson (1996). Super-Resolved Surface Reconstruction from Multiple Images. In Glenn R. Heidbreder, editor, *Maximum Entropy and Bayesian Methods*. Kluwer Academic Publishers.
- Press, W. H., Teukolsky, S. A., Vetterling, W. T., and Flannery, B. P. (2003). *Numerical Recipes in C++: The Art of Scientific Computing*. Cambridge University Press, 2nd edition.
- Reddy, B. and Chatterji, B. (1996). An FFT-based technique for translation, rotation, and scale-invariant image registration. *IEEE Transactions on Image Processing*, 5(8):1266–1271.
- Siavash Zokai and George Wolberg (2005). Image Registration Using Log-Polar Mappings for Recovery of Large-Scale Similarity and Projective Transformations. *IEEE Transactions on Image Processing*, 14(10):1422–1434.
- Tommasini, T., Fusiello, A., Trucco, E., and Roberto, V. (1998). Making good features track better. In *Proceedings of the IEEE Conference on Computer Vision and Pattern Recognition*, pages 178–183, Santa Barbara, CA. IEEE Computer Society Press.
- Tony Lindeberg (1998). Feature Detection with Automatic Scale Selection. *International Journal of Computer Vision*, 30(2):77–116.
- You-Dong Liang and Brian A. Barsky (1983). An analysis and algorithm for polygon clipping. *Communications of the ACM*, 26(11):868–877.